Planetary Crater Detection and Registration Using Marked Point Processes, Multiple Birth and Death Algorithms, and Region-based Analysis

David Solarna[2], Gabriele Moser[2],
Jacqueline Le Moigne[1], and Sebastiano B. Serpico[2]

[1] NASA Goddard Space Flight Center
[2] University of Genoa

IGARSS 2017, Fort Worth, Texas, July 2017

Content

Introduction

Crater Detection

- Marked Point Process Model
- Energy Function
- Multiple Birth and Death Algorithm
- Region-of-Interest Approach
- Experimental Results

Image Registration

- 2-step Approach
- Experimental Results

Conclusion

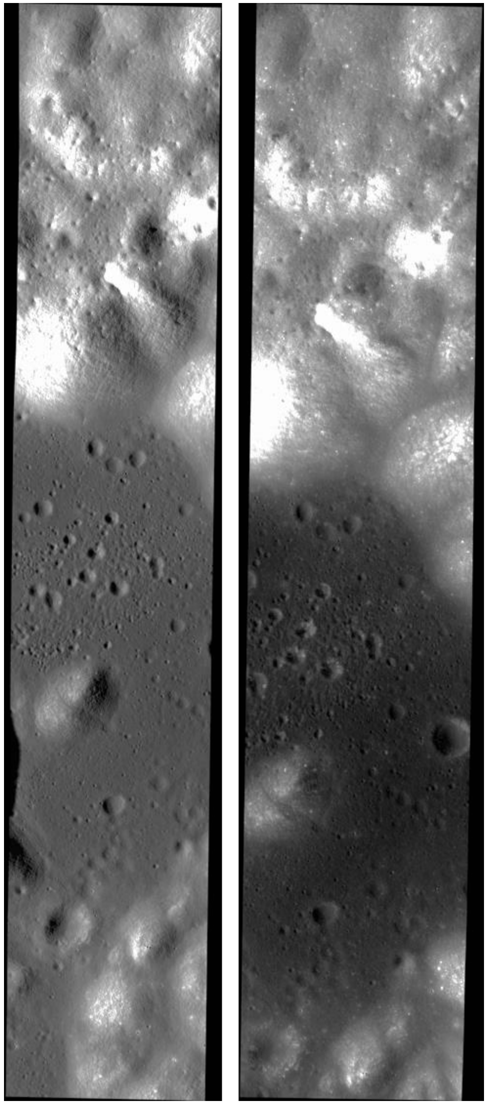

Content

Introduction

Crater Detection

- Marked Point Process Model
- Energy Function
- Multiple Birth and Death Algorithm
- Region-of-Interest Approach
- Experimental Results

Image Registration

- 2-step Approach
- Experimental Results

Conclusion

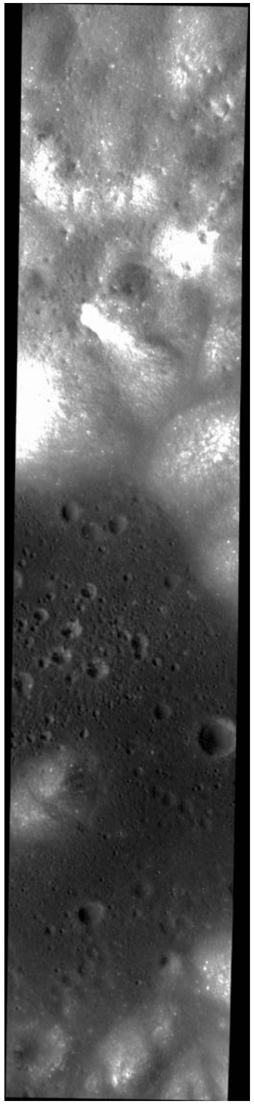

Introduction

Need for automated methods for image registration

Launch of several planetary missions

Design of new and powerful sensors

Large data sets

Multisensor

Multitemporal

Both

Objective

- **Crater detection** in planetary images
- Development of an **image registration** method based on the **extracted features**

Original Data Set

Crater Detection

Crater Map

Crater Detection

Crater Map

Registration

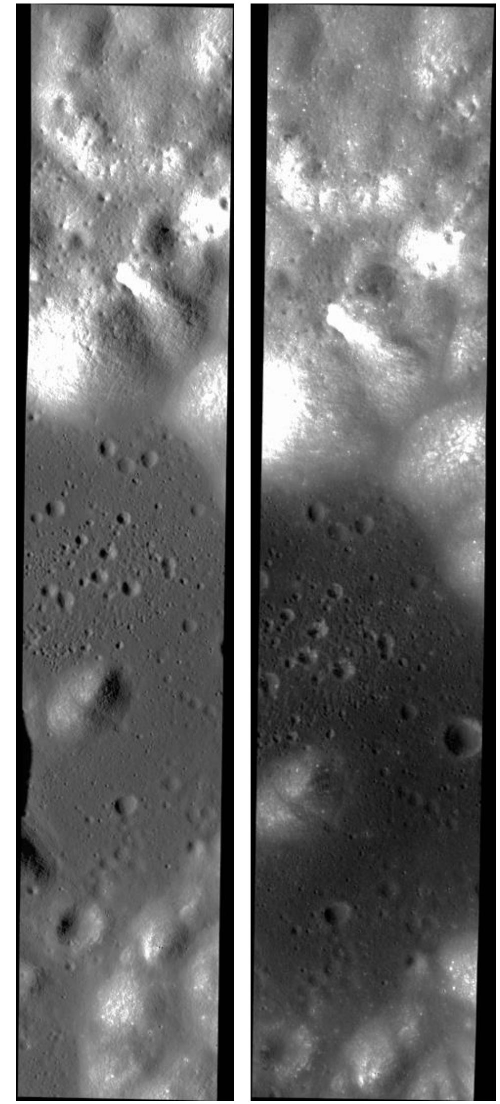

Content

Introduction

Crater Detection

- Marked Point Process Model
- Energy Function
- Multiple Birth and Death Algorithm
- Region-of-Interest Approach
- Experimental Results

Image Registration

- 2-step Approach
- Experimental Results

Conclusion

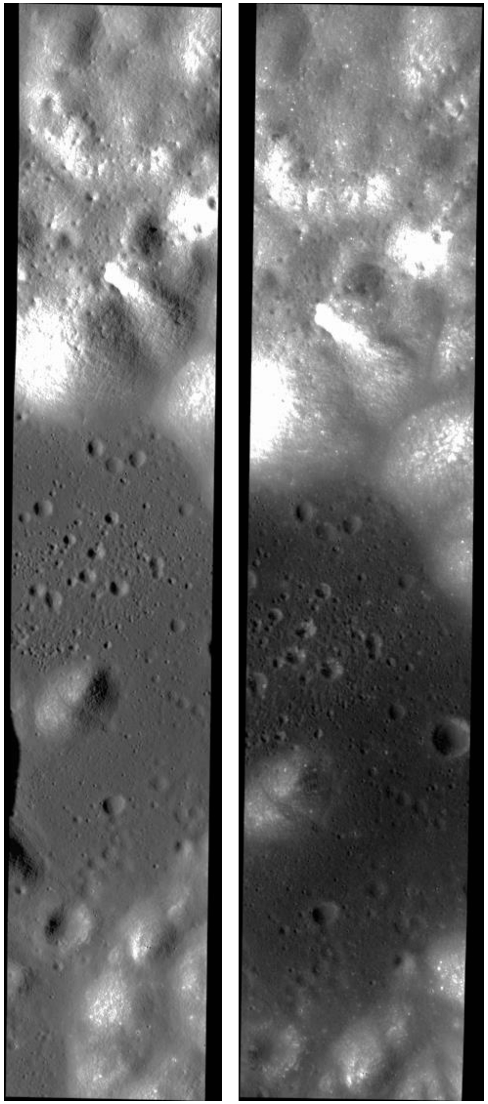

Marked Point Processes

Crater detection based on a marked point process (MPP) model

MPP: Stochastic Process $\xrightarrow{\text{Realizations}}$ Configurations of objects, each described by a marked point

Mathematical Formulation

A **point process** X, defined over a bounded subset P of $\mathbb{R}^2$ maps from a probability space to a **configuration of points** in P.

Realizations of the process X are **random configurations** x **of points**, $x = \{\boldsymbol{x}_1, \dots, \boldsymbol{x}_n\}$, where $\boldsymbol{x}_i$ is the **location** of the i^{th} point in the **image plane** ($\boldsymbol{x}_i \in P$)

A **configuration** of an **MPP** consists of a point process whose **points are enriched with additional parameters**, called **marks** and aimed at parameterizing objects linked to the points.

Bayesian approach: Maximum *a posteriori* (MAP) rule to **fit the model** to the image is equivalent to **minimizing an energy function** (computationally challenging)

Marked Point Process for Crater Detection

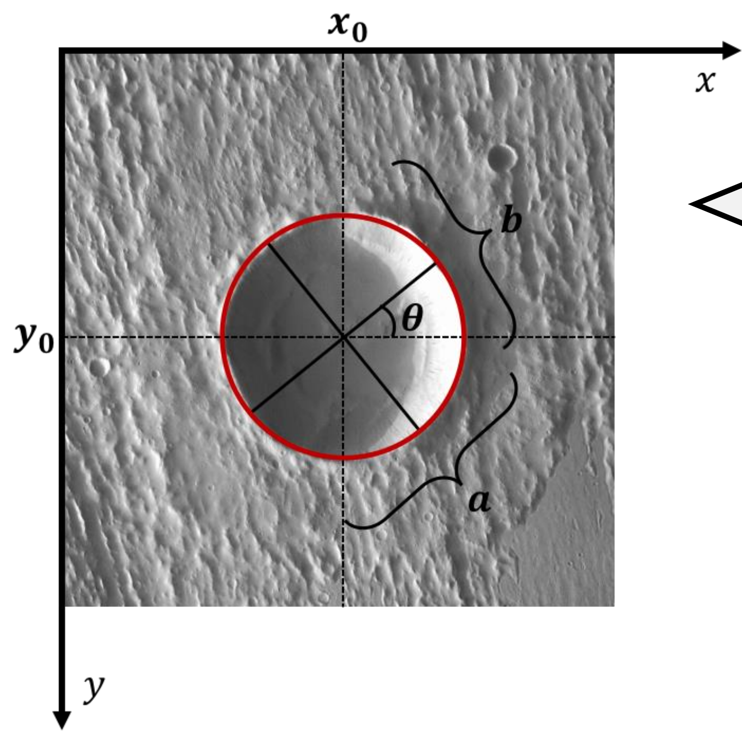

Modelling

Crater → Ellipse

Distribution of craters on the surface → Distribution of ellipses on the image plane

Craters
- Center: (x_0, y_0) } Point
- Major Axis: a
- Minor Axis: b
- Orientation: θ

(Major Axis, Minor Axis, Orientation) } Marks

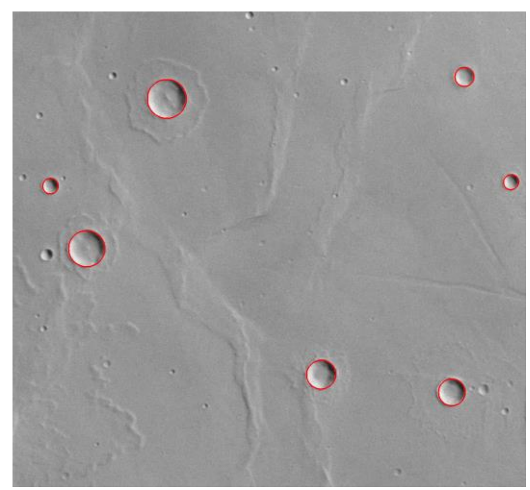

Realization Example

Point Process

$$x = \{\boldsymbol{x}_1, \dots, \boldsymbol{x}_7\}$$

Parameters

$$\boldsymbol{x}_i = (x_{0i}, y_{0i}, a_i, b_i, \theta_i)$$

Crater Detection – Energy Function

Energy function of the configuration $X = \{\boldsymbol{x}_i, \boldsymbol{x}_2, \dots, \boldsymbol{x}_n\}$ wrt the extracted set C of **contour pixels** (Canny):

$$U(X|C) = U_P(X) + U_L(C|X)$$

Prior

Repulsion coefficient based on the overlapping of the ellipses (overlapping craters are quite unlikely)

$$U_P(X) = \frac{1}{n} \sum_{\boldsymbol{x}_i \wedge \boldsymbol{x}_j > 0} \frac{\boldsymbol{x}_i \wedge \boldsymbol{x}_j}{\boldsymbol{x}_i \vee \boldsymbol{x}_j}$$

$\boldsymbol{x}_i \vee \boldsymbol{x}_j$= area of union of ellipses $\boldsymbol{x}_i$ and $\boldsymbol{x}_j$

$\boldsymbol{x}_i \wedge \boldsymbol{x}_j$= area of intersection of $\boldsymbol{x}_i$ and $\boldsymbol{x}_j$

Likelihood

Two terms, one based on a **correlation** measure, the other based on a **distance** measure (fit between contours and realization of X)

$$U_L(C|X) = \sum_{i=1}^{n} \left[\frac{d_{\mathcal{H}}(x_i^0, C)}{n a_i} - \frac{|x_i^0 \cap C|}{|C|} \right]$$

x_i^0 = set of pixels corresponding to ellipse $\boldsymbol{x}_i$ in the image plane

$d_{\mathcal{H}}(x_i^0, C)$ = Hausdorff distance between ellipse $\boldsymbol{x}_i$ and the contours:

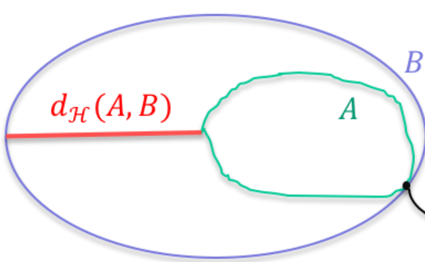

$$d_{\mathcal{H}}(A,B) = \max\left\{ \sup_{\alpha \in A} \inf_{\beta \in B} d(\alpha,\beta) \, ; \, \sup_{\beta \in B} \inf_{\alpha \in A} d(\alpha,\beta) \right\}$$

Classical distance between sets $d(A,B) = 0$

Crater Detection – Energy Minimization

Markov chain Monte Carlo-type method
Simulated Annealing scheme

⇒

Markov chain sampled by a multiple birth and death (MBD) algorithm

Initialization
- **Contour Extraction** (Canny) and Parameter Initialization
- Generation of the **Birth Map** used to speed up the convergence

Birth Step
- Computation of the **Birth Probabilities** for each pixel
- **Birth Phase**

Death Step
- **Energy Computation** for all the ellipses
- Computation of **Death Probability** and **Death Phase** according to **Likelihood**
- **Configuration** refinement according to **Prior**

Update
- **Convergence Test**

MBD – Birth and Death Steps

Birth Step

For **each pixel** s in the image, compute the **birth probability** as $\min\{\delta \cdot B(s), 1\}$, where:

$$B(s) = \frac{b(s)}{\sum_s b(s)}$$

$b(s)$ is the **birth map** computed from the contour map using generalized Hough transform and Gaussian filtering

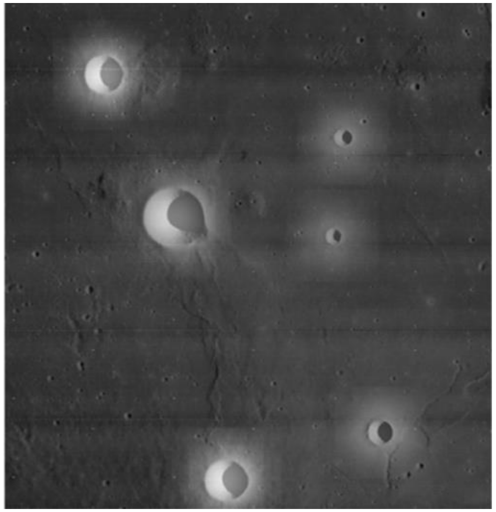

Death Step

For **each ellipse** $\boldsymbol{x}_i$ in the configuration, compute the **death probability** as $d(\boldsymbol{x}_i)$:

$$d(\boldsymbol{x}_i) = \frac{\delta \cdot a(\boldsymbol{x}_i)}{1 + \delta \cdot a(\boldsymbol{x}_i)}$$

$$a(\boldsymbol{x}_i) = \exp\left[-\beta\left(U_L(X\backslash\{\boldsymbol{x}_i\}|C) - U_L(X|C)\right)\right]$$

Crater Detection – Region Based Approach

Region-Based Approach

Why?

- MBD is **computationally heavy**
- Computational burden increases with **image size**

Region Based Flowchart and Example

Initialization

↓

Detection of **regions on interest** based on the birth map

↓

MBD in each **region**

↓

Aggregation

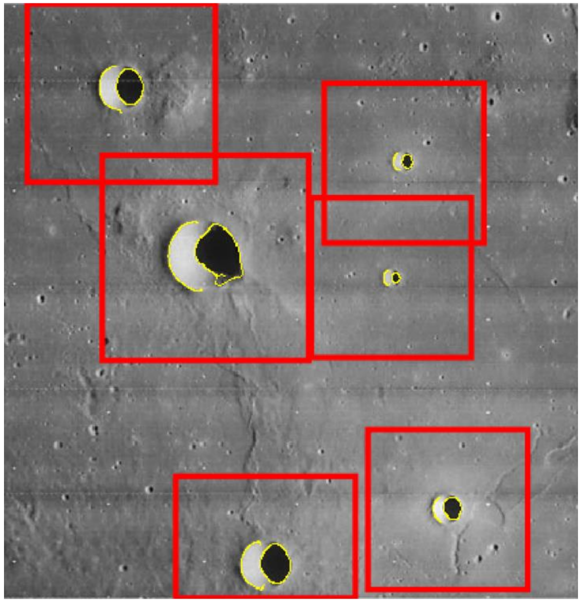

Crater Detection – Data Sets

- 6 THEMIS (Thermal Emission Imaging System) images, TIR, 100m resolution, Mars Odissey mission
- 7 HRSC (High Resolution Stereo Color) images, VIS, ~20m resolution, Mars Express mission
- Image sizes from 1581 × 1827 to 2950 × 5742 pixels

Quantitative Performance Assessment of the crater detection algorithm: Detection Percentage (D), Branching Factor (B), and Quality Percentage (Q)

Data	$D = \frac{TP}{TP + FN}$	$B = \frac{FP}{TP}$	$Q = \frac{TP}{TP + FP + FN}$
Avg on all THEMIS	0.91	0.10	0.83
Avg on all HRSC	0.89	0.06	0.85
Avg on all images	0.90	0.09	0.84

Crater Detection – Results

HRSC Sensor

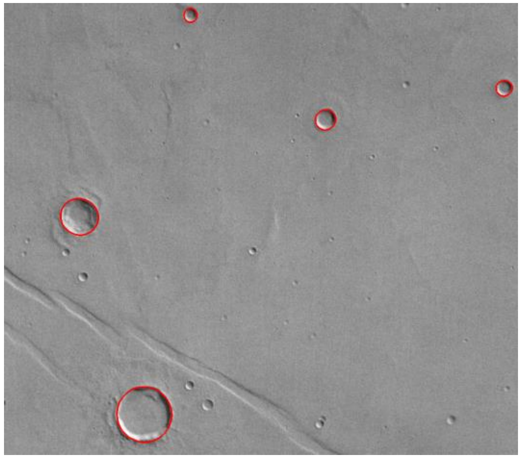

Crater geometric properties extracted by the proposed method			
Crater	$\boldsymbol{C = (x_0, y_0)}$	**Semi-axes** $\boldsymbol{(a, b)}$	**Orientation** $\boldsymbol{\theta}$
Crater 1	$(139, 393)$	$(35, 33)$	$64°$
Crater 2	$(258, 756)$	$(51, 50)$	$115°$
Crater 3	$(343, 23)$	$(13, 12)$	$180°$
Crater 4	$(591, 215)$	$(19, 18)$	$31°$
Crater 5	$(919, 157)$	$(15, 14)$	$106°$

HRSC Sensor

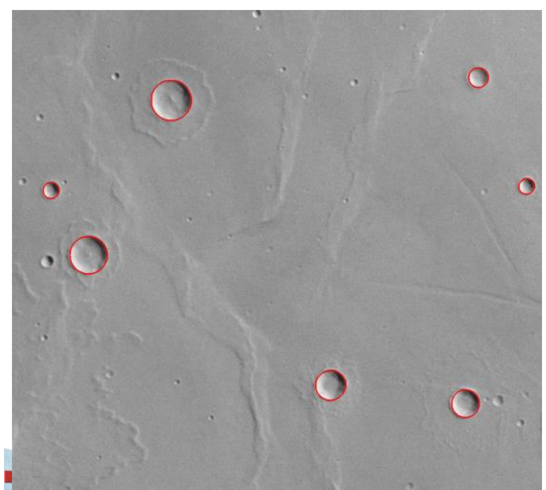

THEMIS Sensor

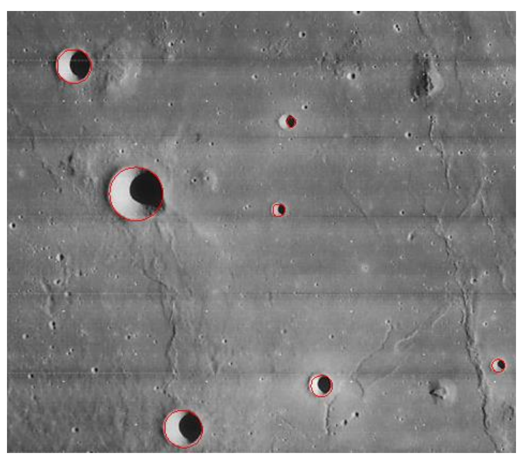

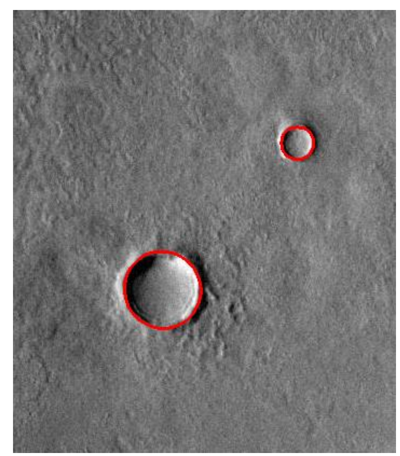

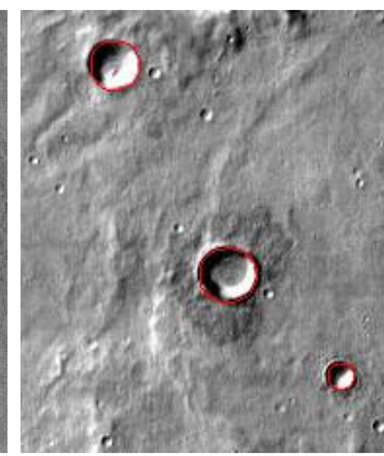

Content

Introduction

Crater Detection

– Marked Point Process Model
– Energy Function
– Multiple Birth and Death Algorithm
– Region-of-Interest Approach
– Experimental Results

Image Registration

– 2-step Approach
– Experimental Results

Conclusion

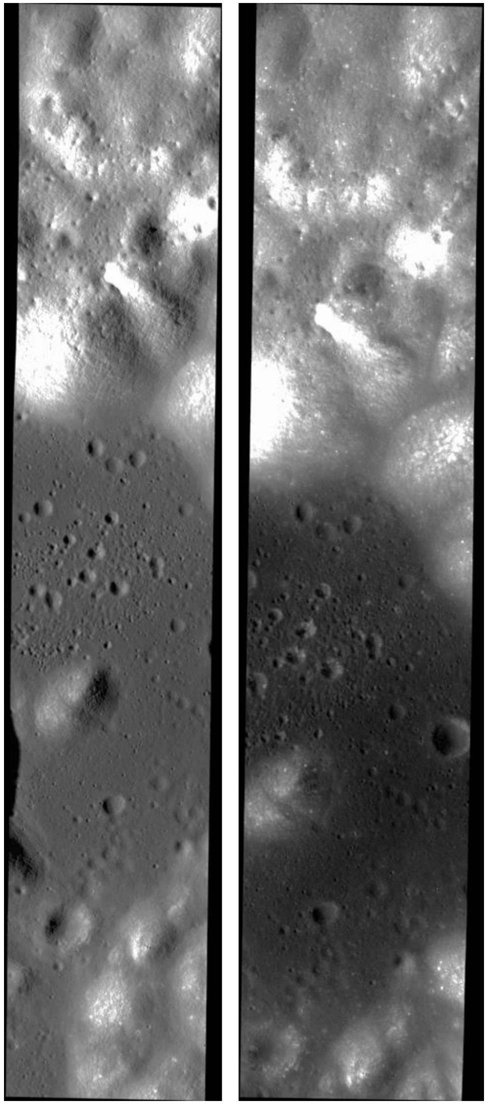

Image Registration – 2-Step Optimization

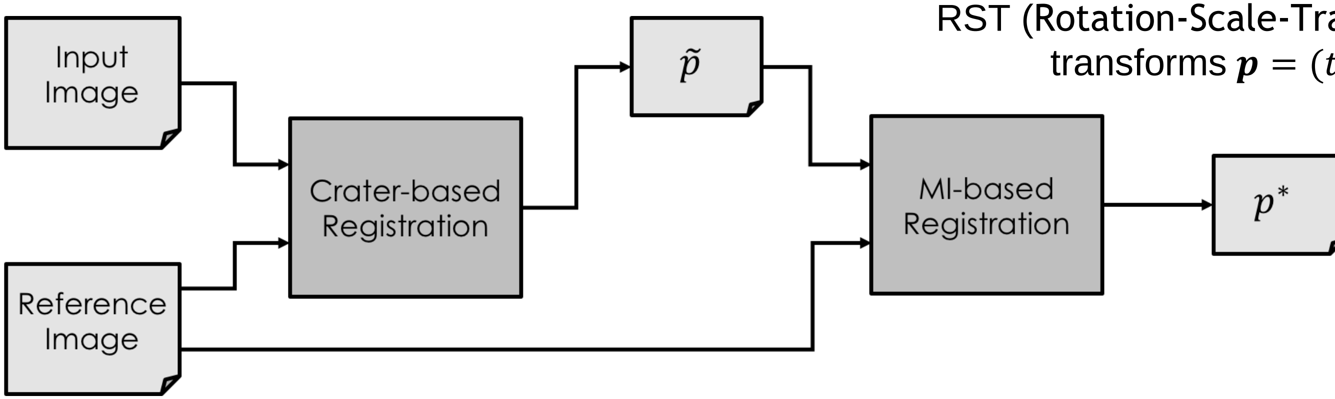

RST (Rotation-Scale-Translation) transforms $\boldsymbol{p} = (t_x, t_y, \theta, k)$

Why a 2-step Optimization?

Feature-based registration
- Min Hausdorff distance ($d_{\mathcal{H}}$) between extracted craters through genetic algorithm
- Fast but sensitive to accuracy of crater maps

Area-based registration
- Max Mutual Information (MI) through genetic algorithm
- Highly accurate but computationally heavy

Initialization

↓

Fast registration based on **extracted craters** → $\tilde{\boldsymbol{p}}$

↓

Refinement: registration based on **mutual information** in a **neighborhood** of $\tilde{\boldsymbol{p}}$ → $\boldsymbol{p}^*$

Image Registration – Region of Interest

Transformation found for an interactively selected region of interest → p_B^*

$p_B = (t_x, t_y, \theta, k)$

Transformation derived for the entire Image → p_A^*

$p_A = (T_x, T_y, \beta, \alpha)$

$$p_A^* = \begin{pmatrix} -k\cos(\theta)\ x_0 - k\sin(\theta)\ y_0 + t_x + x_0 \\ k\sin(\theta)\ x_0 - k\cos(\theta)\ y_0 + t_y + y_0 \\ \theta \\ k \end{pmatrix}$$

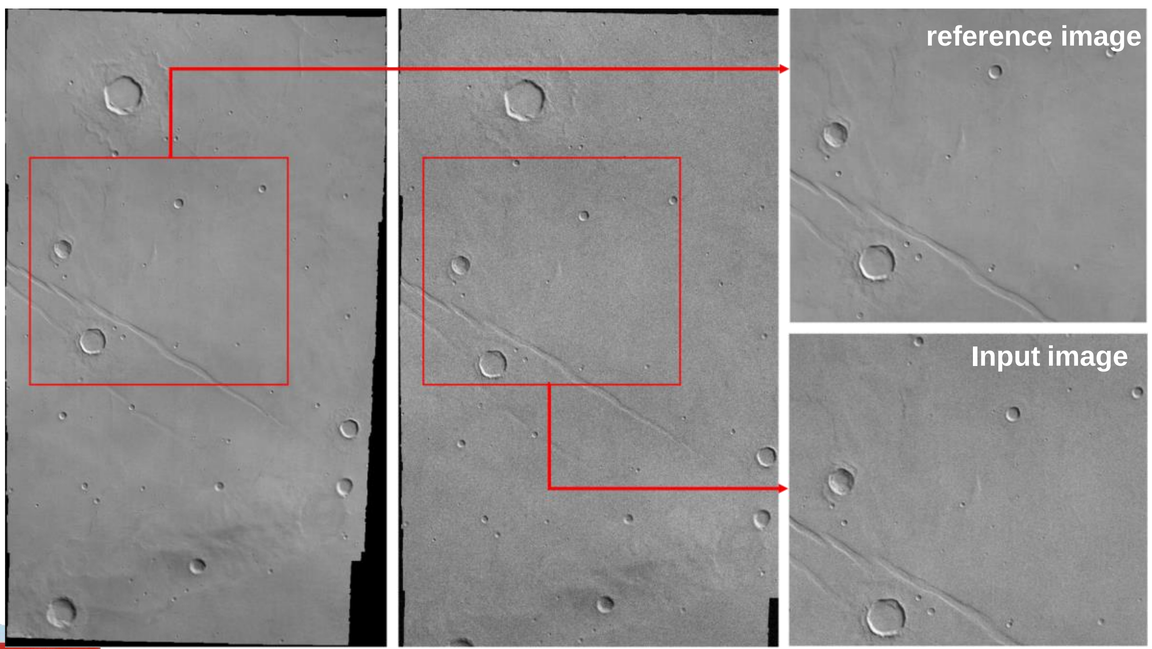

Superposition of Reference and Input

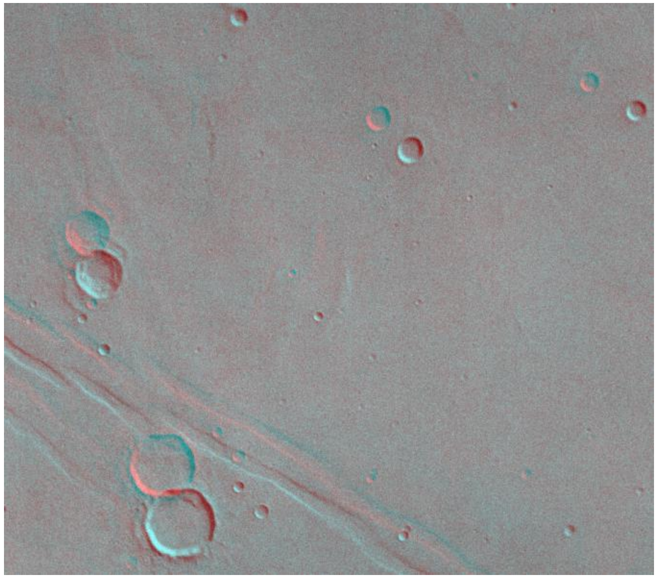

Image Registration – Data Sets

Semi-simulated image pairs

20 pairs composed of one real THEMIS or HRSC image and of an image obtained by applying a synthetic transform and AWGN

Quantitative validation with respect to the true transform (RMSE)

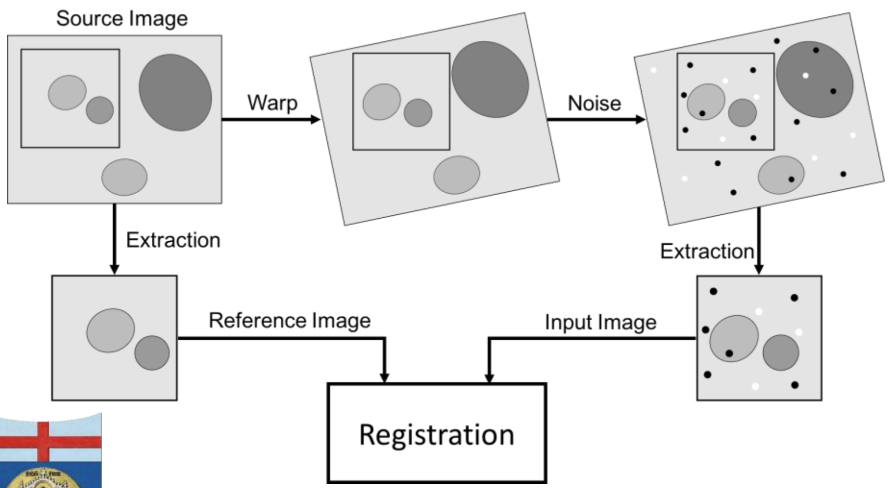

Real multi-temporal image pairs

Real multi-temporal pair of LROC (Lunar Reconnaissance Orbiter Camera) images

100m resolution

Only qualitative visual analysis is available, as no ground truth is available

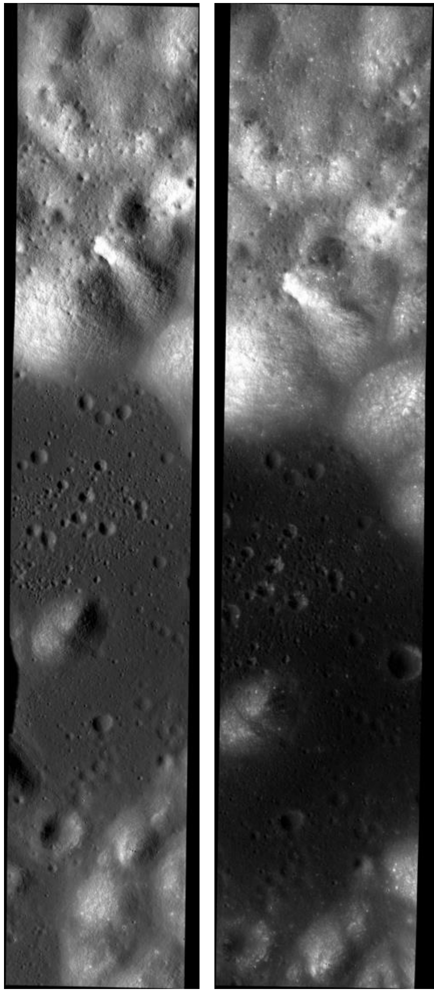

Registration Results with Semi-synthetic Data

RGB of original non-registered data

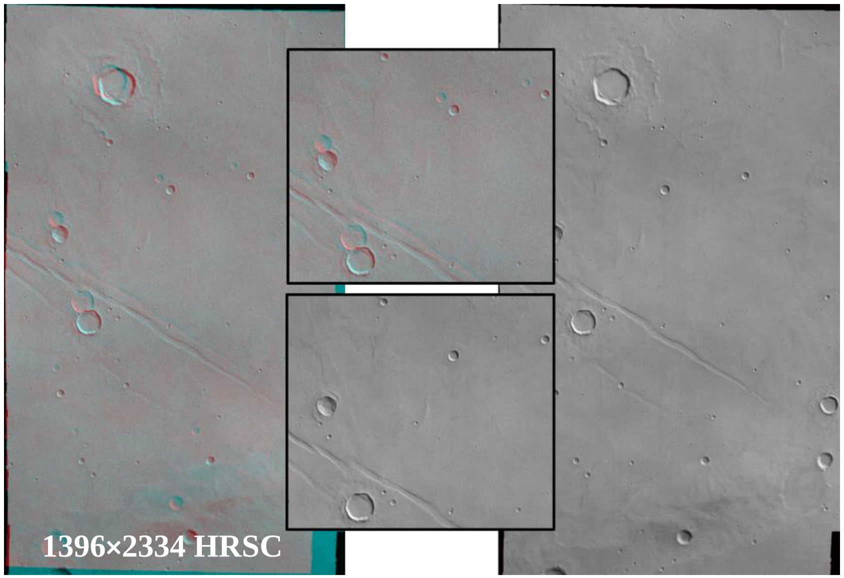

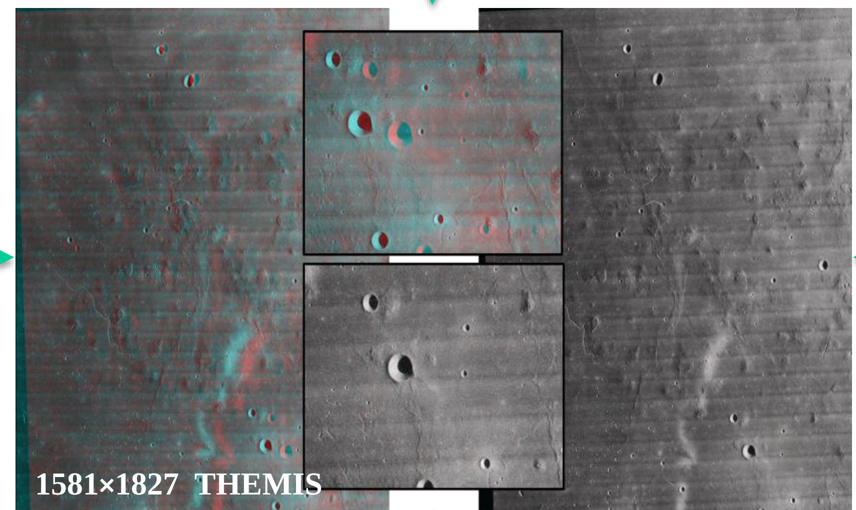

RGB of registered data

Data set	RMSE [pixel]
THEMIS (10 data sets)	0.31
HRSC (10 data sets)	0.22
Average (20 data sets)	0.26

	Left Image	Right Image
p_{GT}	$(7.05, 35.91, 0.18°, 1.071)$	$(76.59, 19.96, 2.17°, 1.031)$
p^*	$(7.04, 35.92, 0.19°, 1.071)$	$(76.41, 20.06, 2.18°, 1.031)$
RMSE 1st Step	0.79	0.51
RMSE 2nd Step	0.16	0.33

Registration Results with Real Data

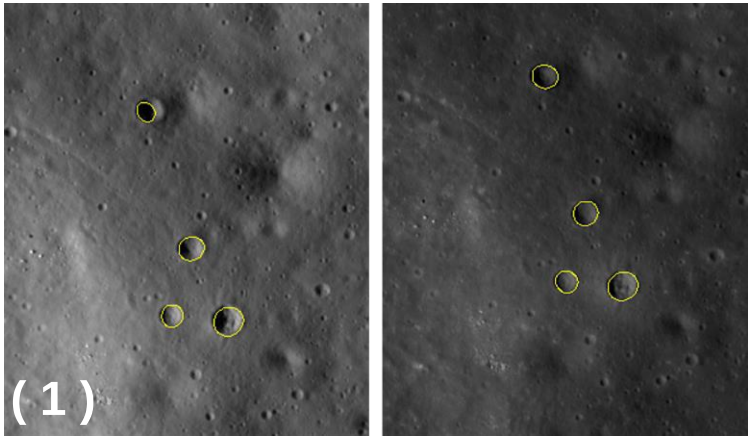

Visually accurate matching between reference and registered images in the real multitemporal data set

Checkerboard representation of the registered images (zoom on details)

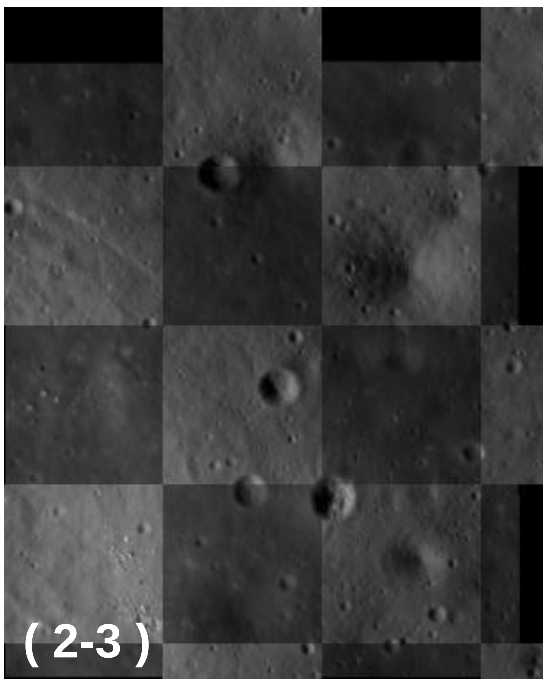

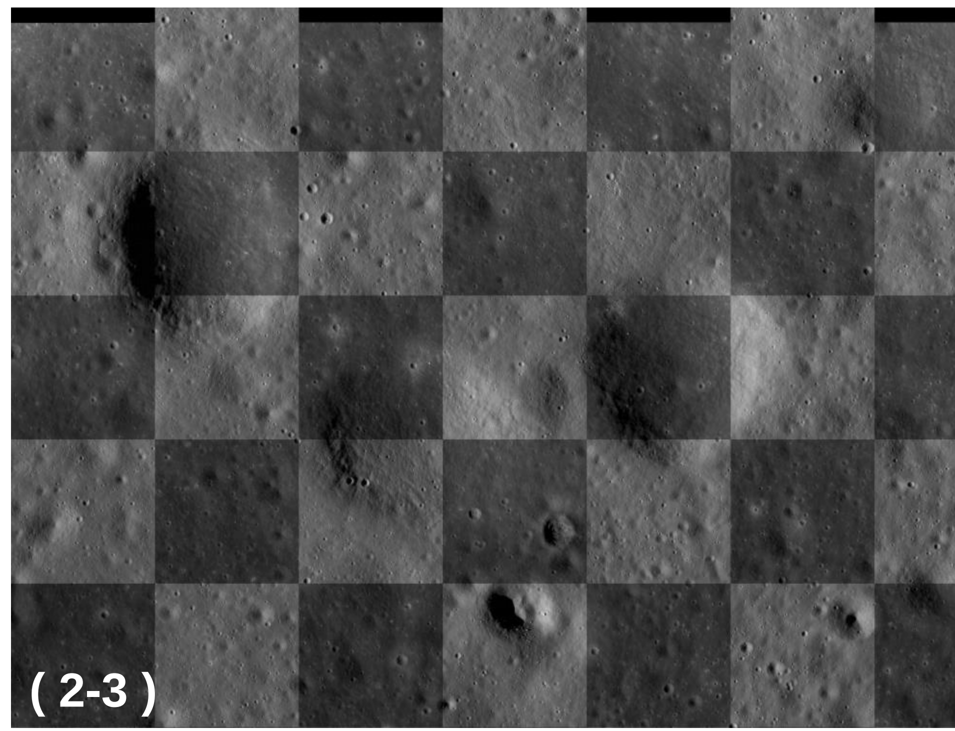

Registration Results with Real Data

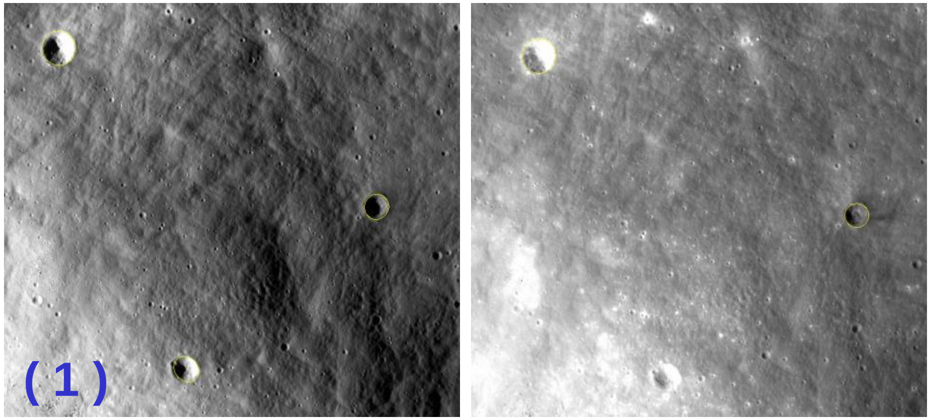

Visually accurate matching between reference and registered images in the real multitemporal data set

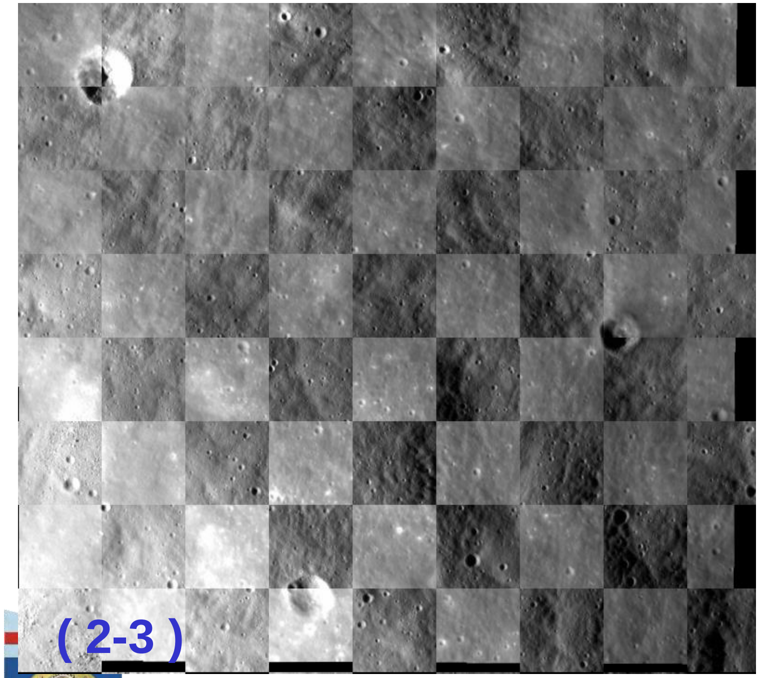

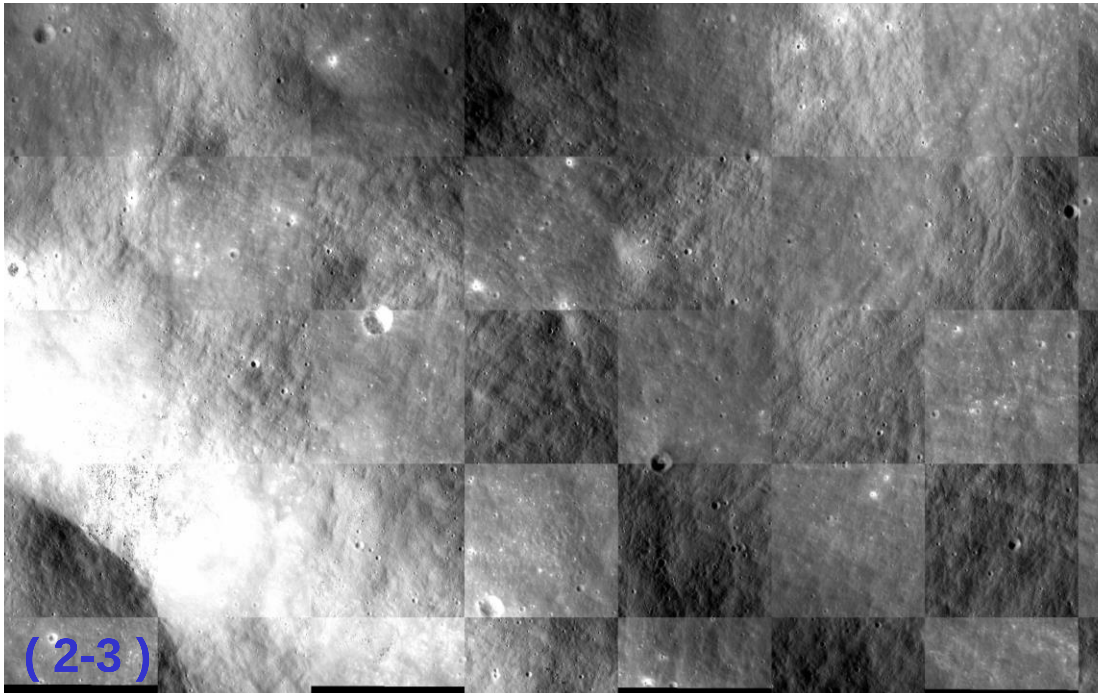

Content

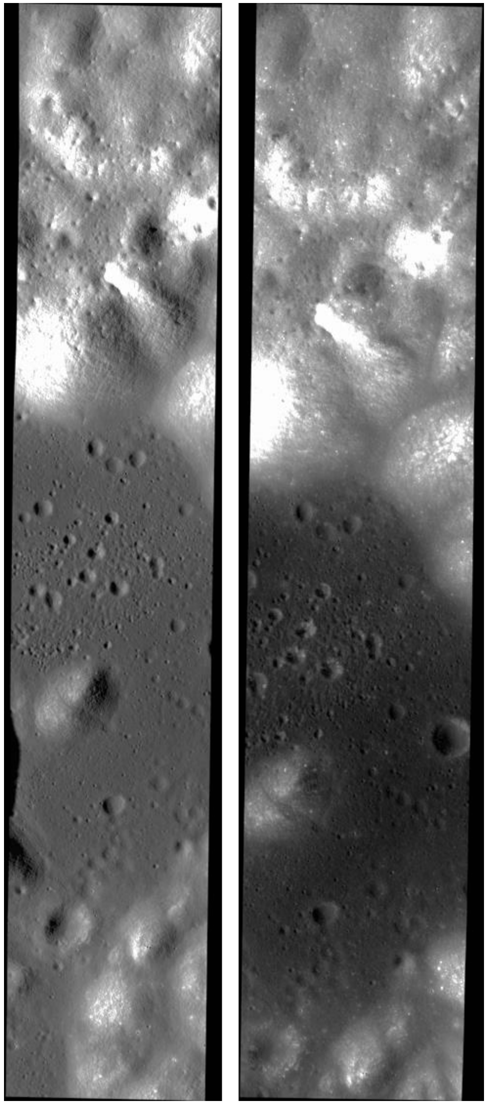

Introduction

Crater Detection

- Marked Point Process Model
- Energy Function
- Multiple Birth and Death Algorithm
- Region-of-Interest Approach
- Experimental Results

Image Registration

- 2-step Approach
- Experimental Results

Conclusion

Conclusions and Future Developments

Conclusions

- **Accurate** crater maps, useful for both image registration and planetary science, were obtained from data from different sensors.
- **Higher accuracy** as compared to previous work on crater detection (not shown for brevity)
- Reduced time for convergence thanks to a **region-based approach**
- **Sub-pixel accuracy and visual precision** in registration: effectiveness of the proposed 2-step registration method

Future Developments

- Test in conjunction with a **parallel** implementation (e.g. computer cluster)
- Validation with **multi-sensor** real images
- Extension to **other applications** requiring the extraction of ellipsoidal or circular features, e.g. optical Earth observation images or medical images

Short Bibliography

- G. Troglio, J. A. Benediktsson, G. Moser and S. B. Serpico, "Crater Detection Based on Marked Point Processes," in *Signal and Image Processing for Remote Sensing*, CRC Press, 2012, p. 325–338.
- G. Troglio, J. Le Moigne, J. A. Benediktsson and G. S. S. B. Moser, "Automatic Extraction of Ellipsoidal Features for Planetary Image Registration," *IEEE Geoscience and Remote Sensing Letters,* vol. 9, pp. 95-99, 2012.
- S. Descamps, X. Descombes, A. Bechet and J. Zerubia, "Automatic Flamingo detection using a multiple birth and death process," in *IEEE International Conference on Acoustics, Speech and Signal Processing*, Las Vegas, NV, 2008.
- X. Descombes, R. Minlos and E. J. Zhizhina, "Object Extraction Using a Stochastic Birth-and-Death Dynamics in Continuum," *Journal of Mathematical Imaging and Vision,* vol. 33, p. 347–359, 2009.
- E. Zhizhina and X. Descombes, "Double Annealing Regimes in the Multiple Birth-and-Death Stochastic Algorithms," *Markov Processes and Related Fields, Polymath,* vol. 18, pp. 441-456, 2012.
- J. Le Moigne, N. S. Netanyahu and R. D. Eastman, Image Registration for Remote Sensing, Cambridge University Press, 2011.
- I. Zavorin and J. Le Moigne, "Use of multiresolution wavelet feature pyramids for automatic registration of multisensor imagery," *IEEE Transactions on Image Processing,* vol. 14, no. 6, pp. 770 - 782, 2005.
- J. M. Murphy, J. Le Moigne and D. J. Harding, "Automatic Image Registration of Multimodal Remotely Sensed Data With Global Shearlet Features," *IEEE Transactions on Geoscience and Remote Sensing,* vol. 54, no. 3, pp. 1685 - 1704, 2016.
- J. H. Holland, Adaptation in natural and artificial systems: an introductory analysis with applications to biology, control, and artificial intelligence, University of Michigan Press, 1975, p. 183.

Appendix

MBD – Birth Step

For **each pixel** in the image compute the **Birth Probability** as $\min\{\delta \cdot B(s), 1\}$, where:

$$B(s) = \frac{b(s)}{\sum_s b(s)}$$

Being $b(s)$ the **Birth Map** computed from the **Canny Contour Map**

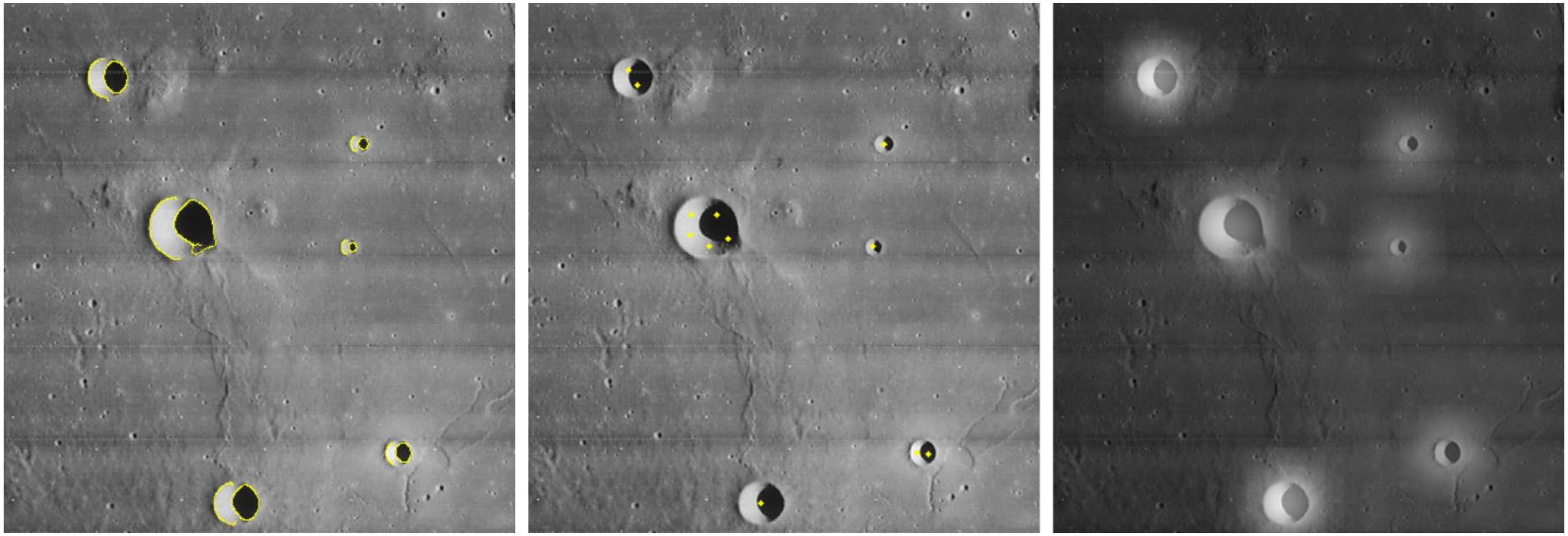

MBD – Death Step

For **each ellipse** x_i in the configuration compute the **Death Probability** as $d(x_i)$, where

$$d(x_i) = \frac{\delta \cdot a(x_i)}{1 + \delta \cdot a(x_i)} \qquad \text{and} \qquad a(x_i) = e^{-\beta\left(U_L(\{x \setminus x_i\}|I_g) - U_L(x|I_g)\right)} = e^{\beta \cdot U_L^i(x_i|I_g)}$$

The complete **Flowchart** of the **Death Step** is as follows:

Computation of the Energy Terms

Computation of Death Prob. based on **Likelihood**

Elimination of ellipses with prob. $d(x_i)$

Configuration refinement thanks to **Prior** term

Similarity Measures

Hausdorff Distance

$$Similarity = mean_c \left\{ \sum_{i=1}^{N^c} \sum_{t=1}^{P} \left[d_H\left(\underline{x}_i^c, \underline{x}_t\right) \right] \right\}$$

$\mathrm{c} = \text{craters in Input Image}$
$\mathrm{N^c} = \text{sum(pixels in crater c in Input Image)}$
$\mathrm{P} = \text{sum(craters'border pixels in Ref Image)}$
$\underline{\mathrm{x}}_\mathrm{i}^\mathrm{c} = \text{coord of pixel i in crater c in Input Image}$
$\underline{\mathrm{x}}_\mathrm{t} = \text{coord of pixel t in Ref Image's craters}$

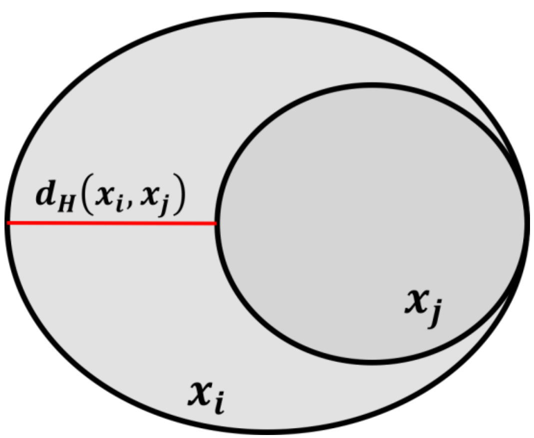

Mutual Information

$$MI(X,Y) = \sum_{x \in X} \sum_{y \in Y} p_{X,Y}(x,y) \log\left(\frac{p_{X,Y}(x,y)}{p_X(x)\, p_Y(y)}\right)$$

X: pixel intensity in Reference Image
Y: pixel intensity in Input Image
$p_X(x)$: probability density function (pdf) of X
$p_Y(y)$: probability density function (pdf) of Y
$p_{X,Y}(x,y)$: joint pdf of X and Y

$p_X(x)$ $\quad$ $p_Y(y)$ $\quad$ $p_{X,Y}(x,y)$

estimated through
the corresponding
image histograms

Rotation – Scale – Translation Transformation

Transformation vector

$$p = (t_x, t_y, \theta, k)$$

$\{t_x, t_y\}$: Translations in x and y

θ: Rotation angle

k: Scaling Factor

Matrix Formulation

$$T_p(x, y) = \begin{pmatrix} k\cos(\theta) & k\sin(\theta) & t_x \\ -k\sin(\theta) & k\cos(\theta) & t_y \end{pmatrix} \begin{bmatrix} x \\ y \\ 1 \end{bmatrix}$$

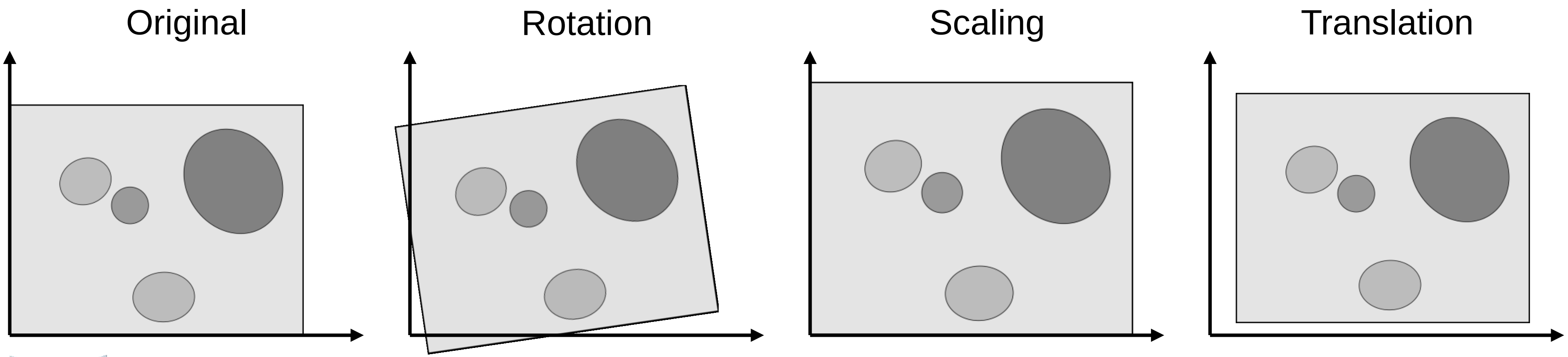

Region of Interest Approach

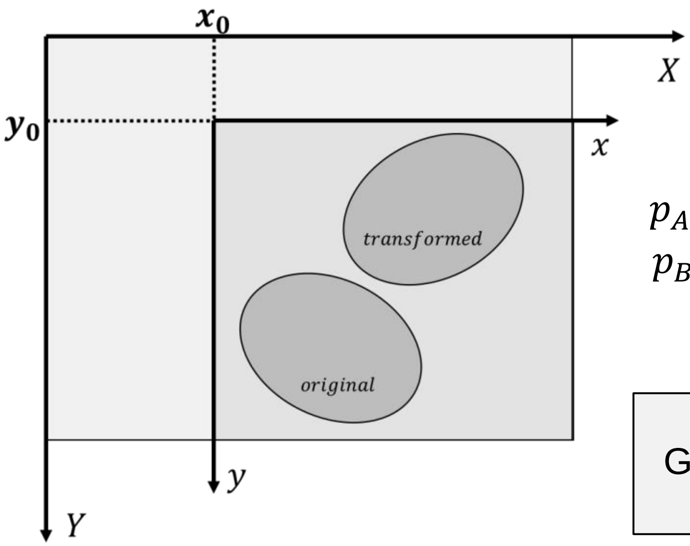

$I_A(X,Y), I_B(x,y)$: Two Images

I_B: sub-image of I_A such that $I_B(0,0) = I_A(x_0,y_0)$

$p_A = (T_x, T_y, \beta, \alpha)$: RST transformation vector transforming I_A into I_A^{tr}

$p_B = (t_x, t_y, \theta, k)$: RST transformation vector transforming I_B into I_B^{tr}

$$I_B^{tr}(0,0) = I_A^{tr}(x_0,y_0)$$

Given: $\begin{cases} Transformation\colon p_B \\ Reference\ of\ Region\colon (x_0,y_0) \end{cases}$ → Find: $Transformation\colon p_A$

From the image

$$\begin{cases} X = x + x_0 \\ Y = y + y_0 \end{cases}$$

Expressing the transformation in Matrix Form

$$T_{p_A} = \begin{pmatrix} \alpha\cos(\beta) & \alpha\sin(\beta) & T_x \\ -\alpha\sin(\beta) & \alpha\cos(\beta) & T_y \end{pmatrix} \ :\ T_{p_A}(X,Y) = (X',Y')$$

$$T_{p_B} = \begin{pmatrix} k\cos(\theta) & k\sin(\theta) & t_x \\ -k\sin(\theta) & k\cos(\theta) & t_y \end{pmatrix} \ :\ T_{p_B}(x,y) = (x',y')$$

This should also hold

$$T_{p_A}(x+x_0, y+y_0) = (x'+x_0, y'+y_0)$$

Plugging T_{p_A} into this equation and replacing x' and y' according to T_{p_B}

$$\begin{cases} k\cos(\theta)\,x + k\sin(\theta)\,y + t_x + x_0 = \\ \alpha\cos(\beta)(x+x_0) + \alpha\sin(\beta)(y+y_0) + T_x \\ \\ -k\sin(\theta)\,x + k\cos(\theta)\,y + t_y + y_0 = \\ -\alpha\sin(\beta)(x+x_0) + \alpha\cos(\beta)(y+y_0) + T_y \end{cases}$$

Knowing $\alpha = k$ and solving in $P_1 = (0,0)$ and $P_2 = (-x_0,-y_0)$

$$p_A = \begin{pmatrix} -k\cos(\theta)\ x_0 - k\sin(\theta)\ y_0 + t_x + x_0 \\ k\sin(\theta)\ x_0 - k\cos(\theta)\ y_0 + t_y + y_0 \\ \theta \\ k \end{pmatrix}$$

RMS Error Computation

Ground Truth Transformation

$$p_{GT} = (t_{x1}, t_{y1}, \theta_1, k_1) \rightarrow T_{p_{GT}}(x,y) = Q_{p_{GT}} \cdot [x,y,1]^T$$

ComputedTransformation

$$p = (t_x, t_y, \theta, k) \rightarrow T_p(x,y) = Q_p \cdot [x,y,1]^T$$

Erorr Transformation

$$p_e = (t_{xe}, t_{ye}, \theta_e, k_e) \rightarrow Q_{P_e} = Q_p \cdot Q_{p_{GT}}^{-1}$$

$$\begin{cases} k_e = \dfrac{k_2}{k_1}, \qquad \theta_e = \theta_2 - \theta_1 \\ t_{xe} = t_{x2} - k_e\left(t_{x1}\cos(\theta_e) + t_{y1}\sin(\theta_e)\right) \\ t_{ye} = t_{y2} - k_e\left(t_{y1}\cos(\theta_e) - t_{x1}\sin(\theta_e)\right) \end{cases}$$

$$(x,y) \in \text{Image}, \ [x', y', 1]^T = Q_{P_e} \cdot [x,y,1]^T$$

$$\begin{bmatrix} x' \\ y' \end{bmatrix} = k_e \begin{pmatrix} \cos(\theta_e) & \sin(\theta_e) \\ -\sin(\theta_e) & \cos(\theta_e) \end{pmatrix} \begin{bmatrix} x \\ y \end{bmatrix} + \begin{bmatrix} t_{xe} \\ t_{ye} \end{bmatrix}$$

RMS Error: $E(p_e) = \sqrt{\frac{1}{AB}\int_0^A \int_0^B (x'-x)^2 + (y'-y)^2 dxdy}, \qquad \alpha = A^2 + B^2$

$$E^2(p_e) = \frac{1}{AB}\int_0^A \int_0^B (k_e \cos(\theta_e)\, x + k_e \sin(\theta_e)\, y + t_{xe} - x)^2 + \left(-k_e \sin(\theta_e)\, x + k_e \cos(\theta_e)\, y + t_{ye} - y\right)^2 dxdy$$

$$E^2(p_e) = \frac{\alpha}{3}(k_e^2 - 2k_e\cos(\theta_e) + 1) + \left(t_{xe}^2 + t_{ye}^2\right) - \left(At_{xe}^2 + Bt_{ye}^2\right)(1 - k_e\cos(\theta_e)) - k_e\left(At_{ye} - Bt_{xe}\right)\sin(\theta_e)$$